Coordination Chemistry Reviews 253 (2009) 1599–1606

Contents lists available at ScienceDirect

Coordination Chemistry Reviews

journal homepage: www.elsevier.com/locate/ccr

Review

Structural effects of tetrachloroauric acid on cell membranes and molecular models

Mario Suwalsky[a,*], Raquel González[a], Fernando Villena[b], Luis F. Aguilar[c], Carlos P. Sotomayor[c], Silvia Bolognin[d], Paolo Zatta[d]

[a] Faculty of Chemical Sciences, University of Concepción, Casilla 160C, Concepción, Chile
[b] Faculty of Biological Sciences, University of Concepción, Concepción, Chile
[c] Institute of Chemistry, Catholic University of Valparaíso, Valparaíso, Chile
[d] CNR Center on Metalloproteins, University of Padova, Padova, Italy

Contents

ARTICLE INFO

Article history:
Received 28 October 2008
Accepted 4 February 2009
Available online 11 February 2009

Keywords:
Gold
Tetrachloroauric acid
Cell membrane
Human erythrocyte
Phospholipid bilayer
Mice brain

ABSTRACT

Gold is a non-essential element extensively used in a variety of applications in medicine. Au(I) compounds have been widely used to treat rheumatoid arthritis, whereas a number of Au(III) derivatives have been prepared and assessed as potential anticancer agents. Gold compounds are well known for their nephrotoxic and neurological implications; however, hematologic toxicity is one of the most serious toxic effects. The lack of information on both neurotoxic and hematotoxic aspects of Au(III) prompted us to study the structural effects of tetrachloroauric acid ($HAuCl_4$) on cell membranes, particularly that of human erythrocytes. In order to better understand the molecular mechanisms of its interaction with cell membranes, a preparation of human red cells and molecular models of the erythrocyte membrane has been used. The molecular models consisted of bilayers of dimyristoylphosphatidylcholine (DMPC) and dimyristoylphosphatidylethanolamine (DMPE), representative of phospholipid classes located in the outer and inner monolayers of the human erythrocyte membrane, respectively. The capacity of $HAuCl_4$ to perturb the bilayer structures of DMPC and DMPE was evaluated by X-ray diffraction, while large unilamellar vesicles (LUVs) of DMPC were analyzed by fluorescence spectroscopy. The effect of $HAuCl_4$ was also examined on the morphology of intact human erythrocytes by scanning electron microscopy (SEM), whereas isolated unsealed human erythrocyte membranes (IUM) were studied by fluorescence spectroscopy. In addition, to better understand gold toxicity in the brain, the effect of a chronic treatment with $HAuCl_4$ is herein reported with immunohistochemical evaluations.

Abbreviations: MLV, multilamellar vesicles; LUV, large unilamellar vesicles; r, fluorescence anisotropy; GP, fluorescence generalized polarization; DPH, 1,6-diphenyl-1,3,5-hexatriene; Laurdan, 6-dodecanoyl-2-dimethylaminonaphthalene; DMPC, dimyristoylphosphatidylcholine; DMPE, dimyristoylphosphatidylethanolamine; SEM, scanning electron microscopy; MT, metallothioneins; GFAP, glial fibrillary acidic protein.

* Corresponding author. Tel.: +56 41 2204171; fax: +56 41 2245974.
E-mail address: msuwalsk@udec.cl (M. Suwalsky).

0010-8545/$ – see front matter © 2009 Elsevier B.V. All rights reserved.
doi:10.1016/j.ccr.2009.02.001

1. Introduction

Gold, in elemental form, has been employed for centuries as an antiprurite to relieve itching palm [1]. In modern medicine, gold therapy (chrysotherapy) of various salts and derivatives in the oxidation state +1 has been widely used, mostly for the treatment of rheumatoid arthritis. Conversely, a number of Au(III) compounds have been prepared and evaluated as potential anticancer agents [2–4]; DNA does not appear to be a primary target for some novel Au(III) compounds even when their cytotoxic effects seem to be mediated by interactions with protein targets [4]. The majority of gold preparations are compounds in which gold is attached to sulfur. The more water-soluble compounds employed in human therapy contain hydrophilic groups as well as the aurothio group. The high affinity for sulfur and the inhibitory effect of gold salts on various enzymes has suggested that the therapeutic effect of gold salts might derive from the inhibition of sulfhydryl systems [1]. A great deal of information is available on gold's toxicology. Gold compounds are well known for their nephrotoxicity further complicated by proteinuria, nephritic syndrome with glomerulonephritis [5]. Neurological complications include myokymia, peripheral neuropathy, Guillain–Barre syndrome, cranial nerve paralysis and encephalopathy [6,7]. Several biochemical properties have also been described, e.g., immunomodulatory effects on the activity of T-cell protein kinase C [8], inhibition of lipopolysaccharide-stimulated tumor necrosis factor-α through the ceramide pathway [9], suppression of the differentiation of human dendritic cells from peripheral blood monocytes [10], and induction of mitochondrial permeability transition [11]. Au(III) has been also reported to oxidize proteins such as insulin and ribonuclease [12]. However, the scarcity of information on the neurotoxic and hematotoxic aspects of Au(III) prompted the study of tetrachloroauric acid ($HAuCl_4$). Au(III) administered as tetrachloroauric acid accumulates only slightly in the brain after a three-month treatment [13]. This result may be indicative of limited permeability: first at the level of the gastrointestinal tract and then at the blood–brain barrier (BBB), which appears to be a very efficient protector [14].

In the course of an *in vitro* systems search for the toxicity screening of chemicals of biological relevance, different cellular models have been applied to examine their adverse effects. The cell membrane is a diffusion barrier that protects the cell interior. Therefore, its structure and functions are susceptible to alterations as a consequence of interactions with chemical species. In order to better understand the molecular mechanisms of the interaction of Au(III) with cell membranes, the effect of $HAuCl_4$ on molecular models of the erythrocyte membranes has been investigated. Erythrocytes were chosen because, although less specialized than many other cell membranes, they share similar functions with them (such as active and passive transport, and the production of ionic and electric gradients) to be considered representative of the plasma membrane in general. The molecular models consisted of multibilayers of dimyristoylphosphatidylcholine (DMPC) and dimyristoylphosphatidylethanolamine (DMPE), and DMPC large unilamellar vesicles (LUVs). DMPC and DMPE are representative of phospholipid classes located in the outer and inner monolayers of the human erythrocyte membrane, respectively [15,16]. The capacity of $HAuCl_4$ to perturb the multibilayer structures of DMPC and DMPE was evaluated by X-ray diffraction while DMPC LUV was analyzed by fluorescence spectroscopy. In an attempt to further elucidate the effect of $HAuCl_4$ on cell membranes, its influence was also examined on the morphology of intact human erythrocytes by scanning electron microscopy (SEM), while isolated unsealed human erythrocyte membranes (IUM) were also studied by fluorescence spectroscopy. These systems and techniques have been previously used to determine the membrane-perturbing effects of other inorganic compounds [17–20]. Morphological alterations in the brain of experimental animals after gold treatment have been reported elsewhere [13]. The conclusion of this study is that Au accumulates slightly in the brain and toxic effects may be observed only at high doses.

2. X-ray diffraction studies of phospholipid multilayers

Despite the wide literature available concerning gold toxicity there are few studies on the interaction between Au(III) and cell membranes and molecular models. One of the few papers concerns the use of bilayers built-up of DMPC and DMPE using X-ray diffraction [13]. Fig. 1A exhibits the results obtained by incubating DMPC with water and $HAuCl_4$. As expected, water altered the structure of DMPC, as its bilayer repeat (phospholipid bilayer width plus the layer of water) increased from about 55 Å in its dry crystalline form [21] to 64.5 Å when immersed in water. Its low-angle reflections (indicated as LA), which correspond to DMPC polar terminal groups, were reduced to only the first two orders of the bilayer repeat. On the other hand, only one strong reflection of 4.2 Å showed up in the wide-angle region (indicated as WA), which corresponds to the average distance between fully extended acyl chains organized with rotational disorder in hexagonal packing. These results were indicative of the gel state reached by DMPC bilayers. Fig. 1A discloses that after exposure to 0.01 mM $HAuCl_4$, there was a slight weakening of DMPC reflection intensities. These considerably decreased with 0.1 mM $HAuCl_4$ and became almost negligible with 3 mM; an effect observed in both the low- and wide-angle DMPC reflections. It can be concluded that $HAuCl_4$ produced a significant structural perturbation, affecting both the polar head and acyl chain regions of DMPC bilayers, and consequently disrupted the in-plane structure and the bilayer stacking. However, as the $HAuCl_4$ concentration increased from 5 to 10 mM, the intensity of the reflection corresponding to the bilayer repeat considerably increased and its observed spacing decreased from 64.5 to 58.8 Å. These effects imply a reordering of DMPC molecules together with a closer approach of the lipid bilayers. Results from similar experiments with DMPE are presented in Fig. 1B. Water significantly affects the bilayer structure of DMPE [21] after the heating–cooling procedure; in fact, it reached the gel state as only two reflections were present, one of 56.4 Å in the low-angle region, and another of 4.2 Å in the wide-angle region. Increasing concentrations of $HAuCl_4$ gradually reduced DMPE reflection intensities; however, all of them were still present with 10 mM $HAuCl_4$, an indication than the extent of the perturbing effect of $HAuCl_4$ was weaker than that induced in the DMPC bilayers.

3. Fluorescence measurements of DMPC LUVs and IUM

The influence of $HAuCl_4$ on the physical properties of DMPC LUVs and IUM was examined by steady-state and time-resolved fluorescence spectroscopy techniques [22–27]. Two fluorescent probes were used, 1,6-diphenyl-1,3,5-hexatriene (DPH) and 6-dodecanoyl-2-dimethylaminonaphtalene (laurdan). DPH fluorescence anisotropy (r) was calculated according to the definition, $r = (I_{||} - I_{\perp})/(I_{||} - 2I_{\perp})$, where $I_{||}$ and $I_{\perp}$ are the corresponding parallel and perpendicular emission fluorescence intensities with respect to the vertically polarized excitation light [22]. Laurdan fluorescence spectroscopic shifts were quantitatively evaluated using generalized polarization (GP) concept [23], which is defined by the expression $GP = (I_b - I_r)/(I_b + I_r)$, where I_b and I_r are the emission intensities at the blue and red edges of the emission spectrum, respectively.

3.1. Steady-state fluorescence measurements

The effect of $HAuCl_4$ incorporation on the properties of DMPC LUV and IUM membranes was studied at 18 and 37 °C on the former and at 37 °C on the latter. Laurdan's emission spectroscopic shifts,

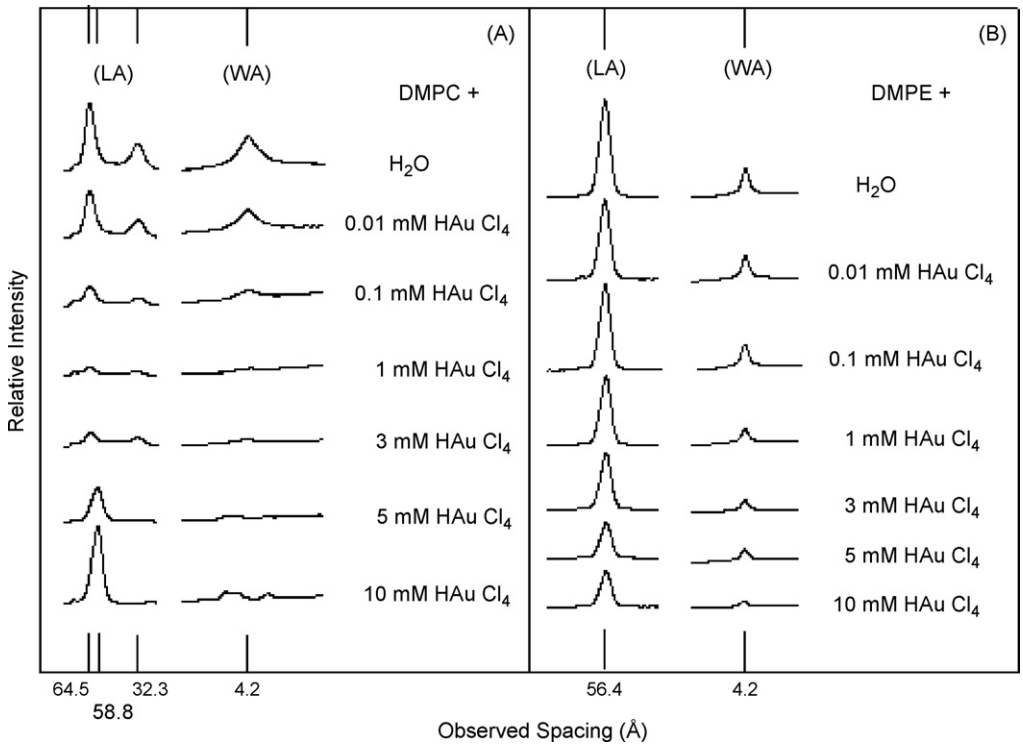

Fig. 1. Microdensitograms from X-ray diffraction diagrams of (A) DMPC and (B) DMPE in water and aqueous solutions of $HAuCl_4$; (LA) and (WA) correspond to low- and wide-angle reflections, respectively.

as a function of the additive concentration and evaluated through the generalized polarization parameter GP, are depicted in Fig. 2. In DMPC LUV membranes, a general tendency characterized by a monotonous increase of GP is observed, being slight at 18 °C and pronounced at 37 °C. In IUM membranes, laurdan GP did not change monotonically with $HAuCl_4$ addition; instead, a trend is apparent with an initial slight decrease up to 0.01 mM followed by an increase up to 0.05 mM, which is then followed by another decrease at the highest measurable concentration. The effects of $HAuCl_4$ incorporation on the steady-state fluorescence anisotropy of DPH embedded in both types of membranes are depicted in Fig. 3. While in DMPC membranes at 18 °C, a slightly steady increase in the anisotropy is observed; at 37 °C, an initial increase with a steep slope occurred up to 0.01 mM followed by a much more gradual increase up to 0.1 mM. On the other hand, in IUM membranes, the anisotropy change followed a general trend analogous to the laurdan GP variation, i.e., an initial decrease, followed by an increase and a further decrease. Interestingly the minima and maxima of both curves occurred at the same $HAuCl_4$ concentrations.

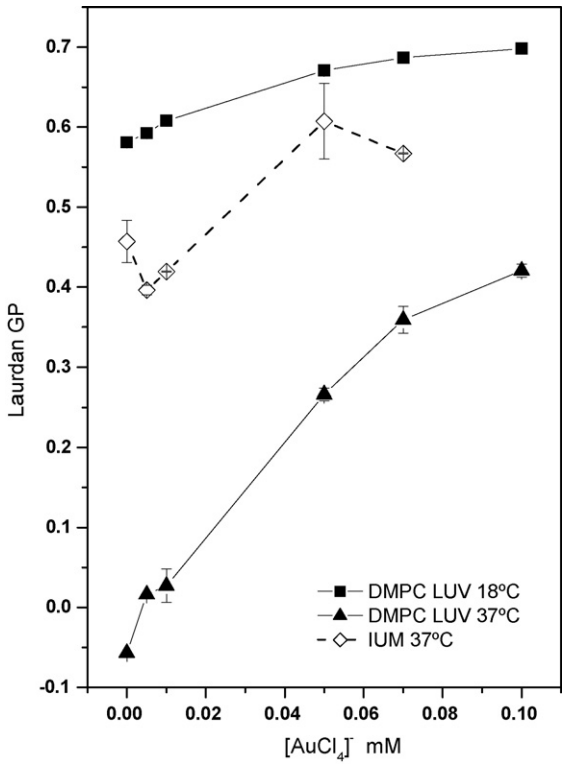

Fig. 2. Effect of $HAuCl_4$ on the generalized polarization (GP) of laurdan in DMPC LUV at 18 and 37 °C and in IUM at 37 °C. Each point represents an average of data in duplicate and standard error.

3.2. Time-resolved fluorescence measurements

Time-resolved fluorescence intensity decay data of DPH embedded in vesicle bilayers was analyzed using different decay models. In all cases, a two-component model consisting of one discrete exponential and one Lorentzian lifetime distribution gave the best fit. A fixed discrete lifetime component of 0.01 ns was used to account for scattered light, which was <2% in terms of fractional intensity contribution. The Lorentzian lifetime distribution center obtained from the analysis is informed as DPH lifetime, and shown in Fig. 4 for DMPC LUVs at 18 and 37 °C, IUM at 37 °C and for DPH dissolved in ethyl alcohol at 18 °C as a control. DPH lifetimes in DMPC LUV without the additive at 18 and 37 °C, 11.14 and 8.72 ns, respectively, are coincident with the reported values for a single lipid bilayer [28,29]. These values did not change significantly with $HAuCl_4$ additions up to 0.01 mM. Over this concentration, significant decreases occurred, although with different trends. At 18 °C, the lifetime decreased with a slight slope up to 0.05 mM, and with a much steeper slope at higher additions. In contrast, at 37 °C, the corresponding decrease occurred with a steep slope up to 0.07 mM, and with a less steep

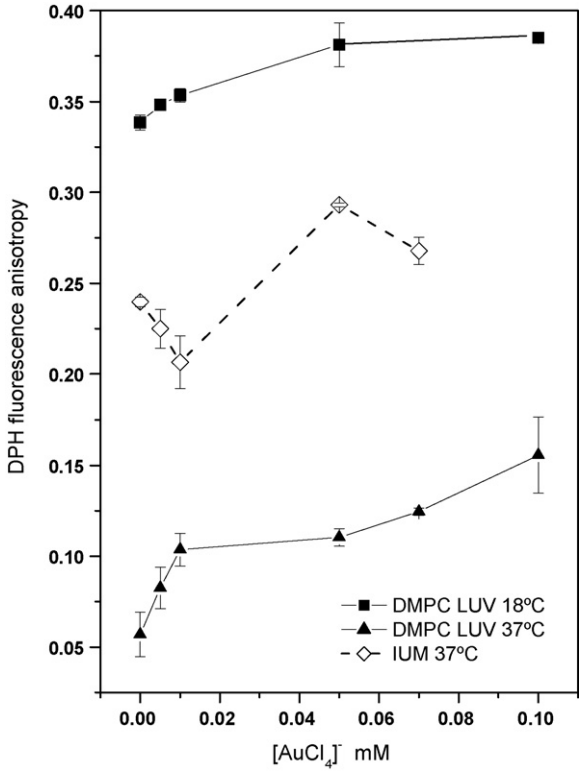

Fig. 3. Effect of $HAuCl_4$ on steady-state fluorescence anisotropy of DPH in DMPC LUV at 18 and 37 °C, and in IUM at 37 °C. Each point represents an average of data in duplicate and standard error.

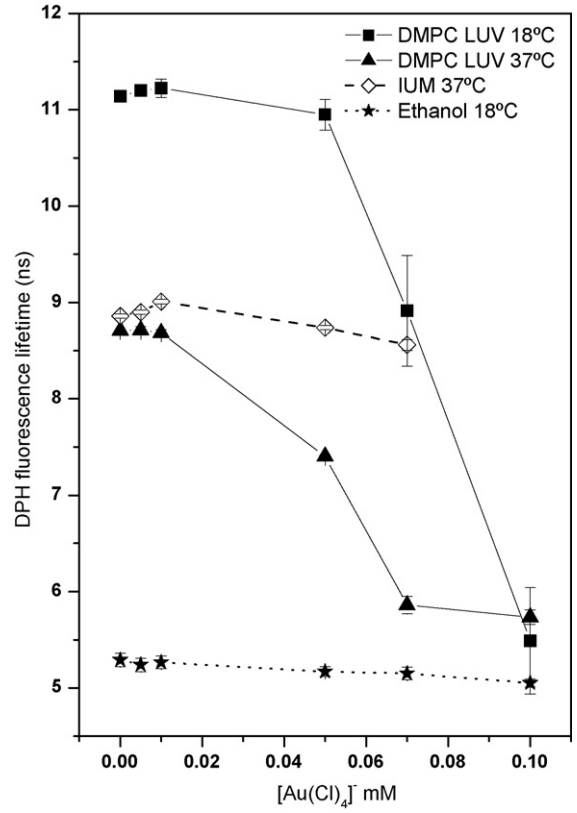

Fig. 4. Effect of $HAuCl_4$ on DPH fluorescence lifetime in DMPC LUV at 18 and 37 °C, in IUM at 37 °C and in ethyl alcohol at 18 °C. Lifetime distribution center obtained from the analysis is depicted as DPH lifetime (see results). The errors represent the correlated 67% confidence limits of the reduced χ^2.

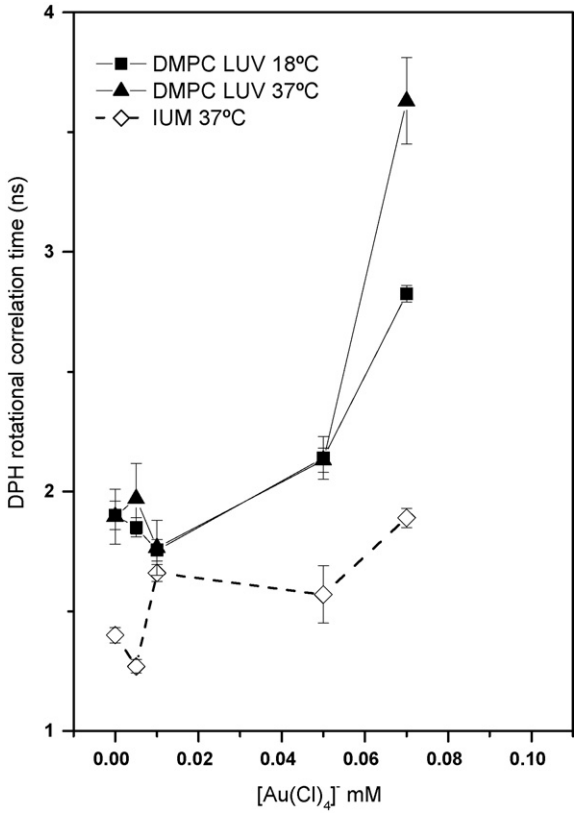

Fig. 5. Effect of $HAuCl_4$ on DPH rotational correlation time in DMPC LUV at 18 and 37 °C, and in IUM at 37 °C. Results were obtained from time-resolved anisotropy decay data, analyzed with a hindered rotator model. The errors represent the correlated 67% confidence limits of the reduced χ^2.

slope at higher concentrations. Noticeably, DPH lifetime at both temperatures was practically coincident at 0.1 mM of $HAuCl_4$. In IUM, DPH lifetime showed a very slight but significant increase up to the addition of 0.01 mM followed by a slight decrease up to 0.07 mM, which is the highest concentration that could be measured. The effect of $HAuCl_4$ addition upon DPH lifetime was also measured in ethyl alcohol in order to establish its quenching capacity over DPH fluorescence. The results indicate that lifetime changes of DPH embedded in the membranes due to $HAuCl_4$ addition cannot be ascribed to its quenching effect.

Time-resolved anisotropy decay data, analyzed with different models, gave the best fit with a hindered rotator model. Rotational correlation times obtained from the analysis, as a function of $HAuCl_4$ concentration, are shown in Fig. 5. In the three cases, a general trend of θ increasing after an initial slight decrease became apparent. The variation tendency was similar for DPH in DMPC LUV at both temperatures. The calculated values of limiting anisotropy, r_∞, in DMPC LUV at 18 °C range from 0.320 (without the additive) up to 0.336 at 0.07 mM $HAuCl_4$, which is, as expected, close to the steady-state fluorescence anisotropy value given in Fig. 3.

4. Scanning electron microscope studies of human erythrocytes

SEM examinations of human erythrocytes incubated with $HAuCl_4$ in the range of 0.1–10 mM indicated that the Au(III) compound $HAuCl_4$ induced changes different from the normal morphology of most red blood cells (Fig. 6). Fig. 6B shows that when incubated with 0.1 mM, numerous cells changed their discoid normal shape into stomatocytes (a cup-shaped form with evagination of one surface and a deep invagination of the opposite face) and

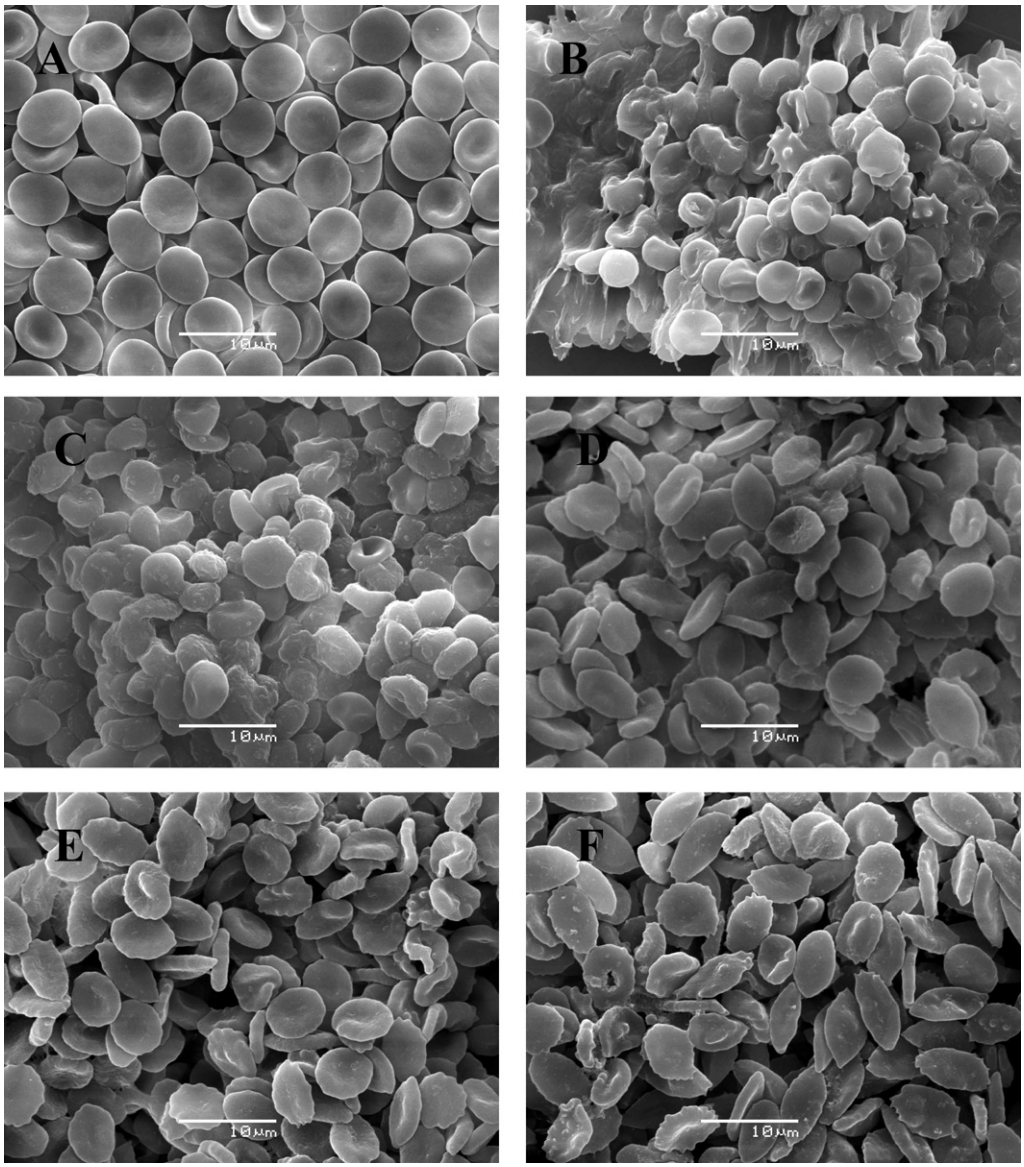

Fig. 6. Effects of $HAuCl_4$ on the morphology of human erythrocytes. Scanning electron microscope images of control (A), and incubated with 0.1 mM (B), 1 mM (C), 3 mM (D), 5 mM (E) and 10 mM $HAuCl_4$ (F).

some into echinocytes (altered condition in which the erythrocytes show a spiny configuration, exhibiting blebs or protuberances in their surfaces); Fig. 6C shows that in 1 mM $HAuCl_4$, most of the cells are spherostomatocytes (cells with a visible change towards spheroid morphology with lightly or minor cupped profiles); 3 mM (Fig. 6D) induced the formation of elliptocytes in most of the cells (cells with an elliptical shape), although some echinocytes did remain; Fig. 6E shows many elliptocytes and some echinocytes when incubated with 5 mM $HAuCl_4$; while with 10 mM (Fig. 6F), most of the cells are elliptocytes, although some knizocytes (red blood cells with two or three concavities due to indentations in the cell membrane) are also observed.

5. Animal toxicity in mice brain after chronic treatment with tetrachloroauric acid

The scarcity of information on gold toxicity prompted the study of its potential effects on brain. In this connection, mice chronically treated with tetrachloroauric acid in drinking water for three months [13] showed a marked alteration in the metallothioneins I–II (MT I–II) and the glial fibrillary acidic protein (GFAP) content with respect to the controls. MTs are a family of low molecular weight proteins which are involved in the detoxification of heavy metals and in the distribution of essential metals. The binding constant of MTs for gold is very high and the metal is able to displace other metal ions such as copper and zinc [30]. In treated animals, a pronounced reduction of MT I–II expression was found in all areas of the brain (Fig. 7). A weak reactivity was found in parts of the cerebellum while other areas, such as the dentate gyrus of the hippocampus, were almost negative. Concomitantly, GFAP expression was reduced in the corpus callosum, fornix and ventral tegmentum of the mesencephalon (Fig. 8) compared to controls. In other areas, immunoreactivity was negligible compared to controls.

6. Concluding remarks

In order to understand the structural effects induced by Au(III) on cell membranes, $HAuCl_4$ was incubated with intact human erythrocytes, their isolated unsealed membranes and bilayers built-up of DMPC and DMPE, which are phospholipid classes present in the

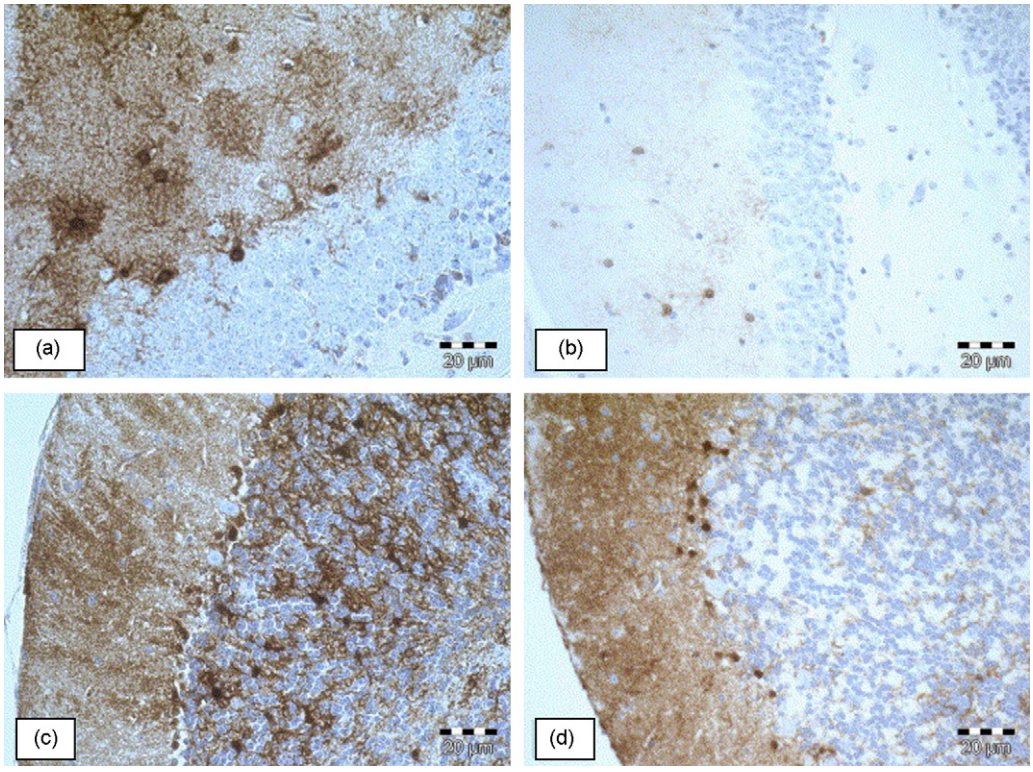

Fig. 7. Immunostaining reactivity to MT I–II in different brain areas; MT I–II positive astrocytes in dentate gyrus of controls (a) and after treatment with $HAuCl_4$ (b), and cerebellar cortex of controls (c) and after treatment $HAuCl_4$ (d) ([13], with permission of Elsevier).

outer and inner monolayers of the erythrocyte membrane, respectively. Analysis by X-ray diffraction showed that concentrations of 0.1 mM and higher $HAuCl_4$ induced structural perturbations of the polar head group and in the hydrophobic acyl regions of DMPC, whose bilayer structure almost completely collapsed with 1 mM $HAuCl_4$. However, concentrations of 3 mM and higher $HAuCl_4$ produced an increase of the first-order reflection intensity together with a decrease of its spacing. The most likely explanation for these

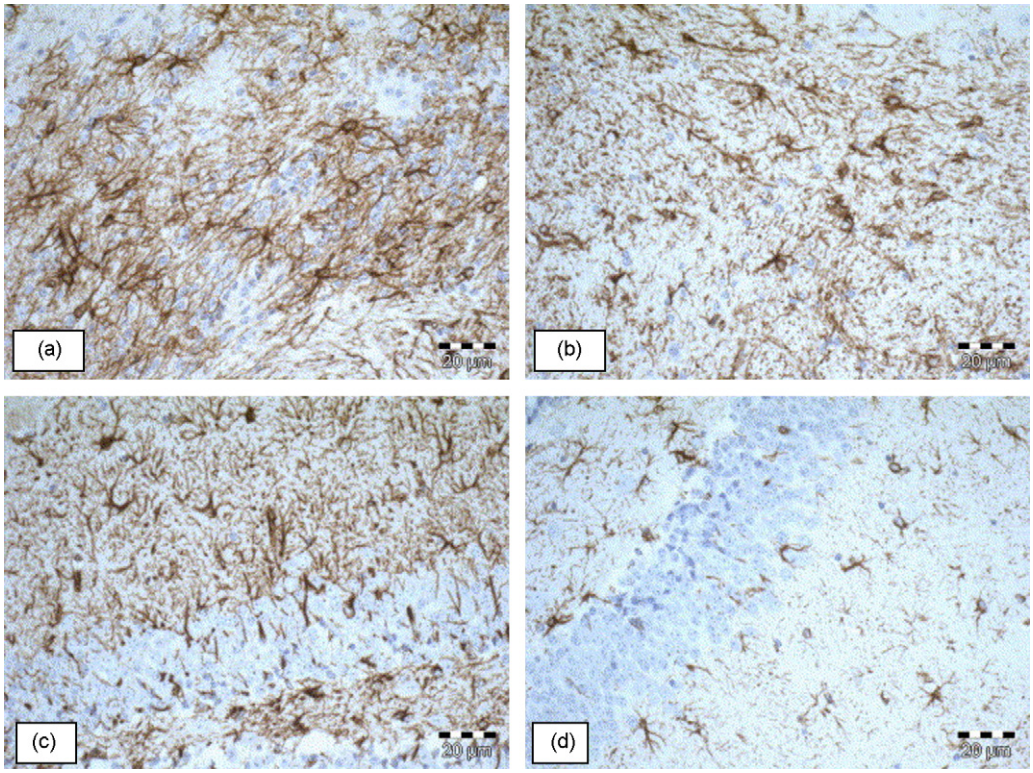

Fig. 8. Immunostaining reactivity to GFAP in different brain areas; GFAP-positive astrocytes in cerebellar medulla of controls (a) and after treatment with $HAuCl_4$ (b) and in dentate gyrus of controls (c) and after treatment with $HAuCl_4$ (d) ([13], with permission of Elsevier).

effects lie in the fact that in the gel state DMPC molecules pack forming the typical bilayer structure with the polar headgroups lying perpendicular to the extended hydrocarbon chains. This arrangement is stabilized through hydrophobic interactions among the acyl chains and electrostatic interactions between the opposite charged PO_4^- and $N(CH_3)^+$ of neighboring headgroups. Water fills the highly polar interbilayer spaces, a condition that promotes the entry of the $AuCl_4^-$ ions. At low concentrations, the relatively scanty $AuCl_4^-$ ions bind electrostatically to a few $N(CH_3)^+$ groups breaking off the stabilizing $PO_4^- \cdots N(CH_3)^+$ interactions inducing a structural perturbation to DMPC. However, at higher $HAuCl_4$ concentrations, $AuCl_4^-$ ions would link to more $N(CH_3)_3^+$ groups of neighboring bilayers. As a result, DMPC bilayers pack closer each other. Similar disorder-order effects have been previously reported for several Al^{3+}, Cu^{2+}, and Fe^{2+} salts [31–33]. When these experiments were repeated with DMPE, only a gradual structural perturbation was observed, and it was much milder than that observed with DMPC. These results can be explained on the basis of the different nature of DMPC and DMPE. Chemically, the two lipids only differ in their terminal amino groups, which are $^+N(CH_3)_3$ in DMPC and $^+NH_3$ in DMPE. Moreover, both molecular conformations are very similar in their dry crystalline phases: their acyl chains are mostly parallel and extended with the polar groups lying perpendicularly to them; however, DMPE molecules pack tighter than those of DMPC. This effect, due to the DMPE smaller polar group and higher effective charge, makes for a very stable multilayer arrangement that was not highly perturbed by $AuCl_4^-$ ions.

Results indicate that fluorescence spectroscopy techniques were suitable for studying the effect of $HAuCl_4$, at low concentrations, on the structural and dynamic properties of lipid membranes. Laurdan and DPH have been selected as probes since they present a number of favorable structural and spectroscopic properties and quite different locations in the bilayer: the hydrophilic–hydrophobic interface near to the polar heads and the deep hydrocarbon region, respectively. The study was performed up to a $HAuCl_4$ concentration of 0.1 mM, and in some cases only up to 0.07 mM due to a considerable decrease of the fluorescence intensity of both probes at these concentrations. In this context, the fluorescence intensity and DPH lifetime were measured in ethyl alcohol as a function of $HAuCl_4$ concentration. Only a slight decrease occurred in DPH lifetime as in its fluorescence intensity, as seen in Fig. 4 for lifetime decrease (intensity data not shown). Thus, $HAuCl_4$ quenching can be ruled out as being responsible for the effects discussed below. The information afforded by laurdan spectroscopic shifts is based on the solvent dipolar relaxation around its fluorophore moiety. Its extent depends both on the solvent's polarity and molecular dynamics, which are quantitatively evaluated using the GP parameter. In a lipid bilayer, the molecules in the probe surroundings responsible for the dipolar relaxation have been determined to be water molecules present at the hydrophobic–hydrophilic interface of the bilayer, near laurdan's fluorescent naphthalene moiety, at the level of the glycerol backbone. Also their concentration is reduced in the gel phase with respect to the liquid crystalline [34]. In this context, the overall GP tendency to increase in DMPC LUV at both temperatures, depicted in Fig. 2, can be ascribed to a reduction in the water content of the hydrophobic–hydrophilic interface and/or in the dynamics of these water molecules due to the interaction of phospholipids polar head groups with $AuCl_4^-$ ions. This effect was larger in the liquid crystalline, at 37 °C, than in the gel state, at 18 °C. In erythrocyte membranes (IUM), a non-monotonical pattern with a minimum at 0.01 mM $HAuCl_4$ and a maximum at 0.07 mM is observed, indicating interactions different from those found in DMPC membranes (see below). Interestingly, the laurdan GP variation patterns in the above-mentioned systems are analogous to their corresponding variation patterns of DPH steady-state fluorescence anisotropy depicted in Fig. 3. Although fluorescence anisotropy is related to fluorophore rotational diffusion, a dynamic event, when it takes place in ordered systems, such as a lipid bilayer, hindered rotations occur due to the orientational constraint imposed by neighboring molecules. In these systems, steady-state fluorescence anisotropy of a fluorophore, such as DPH, is mainly related to the lipid acyl chain packing order, a structural property. The DPH anisotropy variation pattern in DMPC LUV indicates that $HAuCl_4$ addition, at both temperatures, produced an increase in the phospholipids acyl chain packing order, and is larger in the liquid crystalline state, where a substantial increase occurred at low $HAuCl_4$ concentrations, up to 0.01 mM. The resemblance of the DPH fluorescence anisotropy variation trend with the corresponding laurdan GP variation tendency is even greater in IUM: both curves showing minima and maxima at the same $HAuCl_4$ concentrations. Noticeably, both curves showed a decreasing tendency at the highest $HAuCl_4$ concentration attained.

Unexpectedly concomitant DPH lifetimes decreases were found in these systems as shown in Fig. 4. Since DPH lifetime is extremely sensitive to the environment dielectric constant [28], the general tendency of DPH lifetime to decrease with $HAuCl_4$ content is interpreted as an increase in interchain hydration. Interestingly, the DPH lifetime variation trend holds at both temperatures: although they started at different values, both ended at practically the same lifetime value. The difference in DPH lifetimes at 18 and 37 °C, without the additive, is consistent with the difference in membrane water content in the gel and liquid crystalline states [34]. These results indicate that $HAuCl_4$ tends to induce a similar degree of interchain hydration at both temperatures. In IUM, DPH lifetime changes were milder, indicating only slight water content changes. On the other hand, the changes depicted in Fig. 5 for DPH rotational correlation time indicate that a decrease in the fluorophore rotational motion also occurred in the three systems; IUM shows the slightest variation in this parameter. The steady-state and time-resolved fluorescence results are consistent with an effect produced by $HAuCl_4$ in a concentration range up to 0.1 mM. It implies an overall lipid ordering, both at the acyl chain and at polar heads levels; a concomitant increase in the interchain hydration at the hydrophobic core; and a corresponding decrease at the polar head groups level. It also slowed down the molecular rotational diffusion at the phospholipids acyl chain level. A difference in the extent of the $HAuCl_4$ effect induced in DMPC LUV and in IUM is conspicuously apparent in time-resolved measurements. In biological membranes, an important fact to be taken into account is that they have a heterogeneous structure and a complex biochemical composition, which includes different kinds of phospholipids, neutral lipids such as cholesterol, glycolipids and proteins that modify the bilayer properties and interactions.

The fluorescence spectroscopy results on DMPC LUV at 18 °C differ from those obtained by X-ray diffraction, where a disorder effect was attained in the 0.01–1 mM range. The explanation for this discrepancy might lie in that the two systems are different. In fact, the X-ray experiments were carried out in DMPC multibilayers which are relatively more ordered than the unilamellar vesicles used in the fluorescence. In the latter case, $AuCl_4^-$ ions might become inserted in the hydrophilic–hydrophobic interface, inducing a moderate ordering of the polar heads and the deep hydrocarbon regions.

The scanning electron microscopy observations of human erythrocytes incubated with $HAuCl_4$ indicated that they underwent morphological alterations with increasing $HAuCl_4$ concentrations since they changed their normal discoid shape to stomatocytes, echinocytes, elliptocytes and knizocytes. According to the bilayer-couple hypothesis [35], shape changes are induced in red cells due to the insertion of foreign species in either the inner or the outer monolayer of the erythrocyte membrane. Thus, cup-shaped stomatocytes are produced in the first case, while speculated

shapes (echinocytes) are observed in the second due to the differential expansion of the corresponding monolayer. Given the extent of the interaction of $HAuCl_4$ with DMPC and that the lipid class is preferentially located in the outer monolayer of the erythrocyte membrane echinocytes were expected from the erythrocytes incubated with $HAuCl_4$. Although echinocytes were indeed observed, stomatocytes and elliptocytes were more numerous at low and high $HAuCl_4$ concentrations, respectively. The morphological change in stomatocytes might be due to the interaction of $HAuCl_4$ molecules with lipids and/or proteins located in the inner monolayer of the erythrocyte membrane; at higher concentrations, the molecules located in both monolayers produce elliptocytes.

In the brain, gold seems to accumulate prevalently in astrocytes and in a lesser extent in neurons [14]. Nevertheless, the BBB appears to be an efficient protection from gold neurotoxicity since toxic effects may occur only at high gold doses. Histopathological staining of the brain tissue revealed the existence of a population of specialized iron-containing glia, distributed in the hypothalamus *area postrema*, most sensitive to gold thioglucose [36]. Further studies on this issue will definitely lead to a wider understanding of gold neurotoxicology and pharmacology in relation also to the chemical state and nature of the used gold compounds.

7. Summary

Despite the widespread use of Au in a variety of medical applications there is scant information regarding its interaction with cell membranes. Our results indicate that the interaction of $HAuCl_4$ with lipid bilayers perturbs their molecular structures. Since the lipid bilayer is the membrane's main permeability barrier, the structural perturbation induced by $HAuCl_4$ will affect its permeability. It might also affect the functions of ion channels, receptors and enzymes immersed in the membrane lipid moiety. These observations may provide a new insight into the possible mechanism for Au(III) toxicity at the cell membrane level, particularly for human erythrocytes. This is of particular interest since one of the most serious toxic effects of parenteral gold compounds is haematological toxicity [37].

Acknowledgements

The authors thank Prof. Luigi Messori for providing $HAuCl_4$, Fernando Neira for technical assistance, and FONDECYT for research grant 1060990.

References

[1] A. Burke, E. Smyth, G.A. FitzGerald, Analgesic–Antipyretic Agents; Pharmacotherapy of Gout––Goodman & Gilman's The Pharmacological Basis of Therapeutics, 11th ed., McGraw-Hill, 2005, p. 706.
[2] E.R.T. Tiekink, Oncol. Hematol. 42 (2002) 225.
[3] B. Desoize, Anticancer Res. 24 (2004) 1529.
[4] A. Casini, C. Hartinger, C. Gabbiani, E. Mini, P.J. Dyson, B.K. Keppler, L. Messori, J. Inorg. Biochem. 102 (2008) 564.
[5] R. Goyer, Toxic Effects of Metals––Casarett and Doull's Toxicology: The Basic Science of Poisons, MacMillan, 1986, pp. 582–635.
[6] A.G. Fam, D.A. Gordon, J. Sarkozi, G.R. Blais, P.W. Cooper, M. Harth, A.J. Lewis, J. Rheumatol. 11 (1984) 700.
[7] J.A. Garrido, M.V. Rorres-Pardo, D. Solá, C. Marsal, A. Alvarez, A. Lozano, Neurología 10 (1995) 235.
[8] K. Hashimoto, C.E. Whitehurst, T. Matsubara, K. Hirohaka, P.E. Lipsky, J. Clin. Invest. 89 (1992) 1839.
[9] A. Kumar-Mangalam, A. Aggarwal, S. Naik, Cell Immunol. 219 (2002) 1.
[10] Z.Y. Wang, A. Morinobu, S. Kawano, J. Saegusa, B. Wang, S. Kumagai, Clin. Exp. Rheumatol. 20 (2002) 683.
[11] M.P. Rigobello, G. Scutari, R. Rosolo, A. Bindoli, Br. J. Pharmacol. 136 (2002) 1162.
[12] C.F. Shaw, Gold–Gold, Progress in Chemistry, Biochemistry and Technology, Wiley, 1999, pp. 291–292.
[13] M. Suwalsky, P. Zambenedetti, E. Carpené, M. IbnLkayat, W. Wittkowski, L. Messori, P. Zatta, J. Inorg. Biochem. 98 (2004) 2080.
[14] G. Danscher, Histochem. Cell Biol. 117 (2002) 447.
[15] J.M. Boon, B.D. Smith, Med. Res. Rev. 22 (2002) 251.
[16] P.F. Devaux, A. Zachowsky, Chem. Phys. Lipids 73 (1994) 107.
[17] M. Suwalsky, P. Fierro, F. Villena, C.P. Sotomayor, Biophys. Chem. 129 (2007) 36.
[18] M. Suwalsky, C. Rivera, F. Villena, C.P. Sotomayor, M. Jemiola-Rzeminska, K. Strzalka, Biophys. Chem. 127 (2007) 28.
[19] M. Suwalsky, F. Villena, B. Norris, M.A. Soto, C.P. Sotomayor, L. Messori, P. Zatta, J. Inorg. Biochem. 99 (2005) 764.
[20] M. Suwalsky, F. Villena, B. Norris, F. Cuevas, C.P. Sotomayor, J. Inorg. Biochem. 98 (2004) 1061.
[21] M. Suwalsky, Phospholipid Bilayers––Polymeric Materials Encyclopedia, CRC Press, 1996, p. 5073.
[22] J.R. Lakowicz, Principles of Fluorescence Spectroscopy, Plenum, 1999.
[23] T. Parasassi, E. Gratton, J. Fluoresc. 5 (1995) 59.
[24] R.D. Spencer, G. Weber, Ann. N.Y. Acad. Sci. 158 (1969) 361.
[25] E. Gratton, D.M. Jameson, R.D. Hall, Annu. Rev. Biophys. Bioeng. 13 (1984) 105.
[26] J.R. Alcala, E. Gratton, F.G. Prendergast, Biophys. J. 51 (1987) 587.
[27] D.M. Jameson, T.L. Hazlett, Time-resolved Fluorescence Measurements in Biology and Biochemistry––Biophysical and Biochemical Aspects of Fluorescence Spectroscopy, Plenum, 1991, pp. 105–133.
[28] C. Zannoni, A. Arcioni, P. Cavatorta, Chem. Phys. Lipids 32 (1983) 179.
[29] R. Fiorini, M. Valentine, S. Wang, M. Glaser, E. Gratton, Biochemistry 26 (1987) 3864.
[30] K. Saito, K. Yoshida, Res. Commun. Mol. Pathol. Pharmacol. 100 (1998) 83.
[31] M. Suwalsky, B. Norris, T. Kiss, P. Zatta, Coord. Chem. Rev. 228 (2002) 285.
[32] M. Suwalsky, B. Ungerer, L. Quevedo, F. Aguilar, C.P. Sotomayor, J. Inorg. Biochem. 70 (1998) 233.
[33] M. Suwalsky, F. Martínez, H. Cárdenas, J. Grzyb, K. Strzalka, Chem. Phys. Lipids 134 (2005) 69.
[34] T. Parasassi, G. Ravagnan, R.M. Rusch, E. Gratton, Photochem. Photobiol. 57 (1993) 403.
[35] M.P. Sheetz, S.J. Singer, Proc. Natl. Acad. Sci. U.S.A. 75 (1974) 4457.
[36] J.K. Young, Brain Res. Bull. 22 (1989) 929.
[37] American Hospital Formulary Service – Drug Information, 2003.